

EXTERNAL FORCE-FIELD INDUCED CRYSTALLIZATION OF AMORPHOUS MATERIALS: MOLECULAR DYNAMICS STUDY

S.H. Park

Department of Mechanical and System Design Engineering, Hongik University, Seoul, Korea

H.J. Kim

School of Chemical Engineering and Material Science, Hongik University, Seoul, Korea

J.S. Lee

**** School of Mechanical and Aerospace Engineering, Seoul National University, Seoul, Korea*

Y.K. Choi

School of Mechanical Engineering, Chung-Ang University, Seoul, Korea

This is the first investigation on the possibility of the isothermal crystallization induced by an external force-field using molecular dynamics simulation. External cyclic forces with a dc bias are superimposed on the intermolecular forces, which govern the global behavior of molecules. It is discovered that field-enhanced movements of susceptor molecules can induce crystallization effectively without heating problem, the crystallization process becomes more efficient when the external cyclic force is shifted by a dc bias, a radial distribution function is a sufficient tool to observe the progress of the crystallization and the optimal values for the external forces are close to the averaged intermolecular forces.

The authors gratefully acknowledge the financial support from the Micro Thermal System Research Center sponsored by the Korean Science and Engineering Foundation.

Address correspondence to S.H. Park, Department of Mechanical and System Design Engineering, Hongik University, 72-1 Sangsoodong, Mapoku, Seoul 121-791, Korea. E-mail: spark@hongik.ac.kr

The objective in this study is to investigate the isothermal crystallization of an amorphous material induced by external force-fields, using the molecular dynamics (MD) simulation technique. It is assumed that an external sinusoidal force field with a dc bias is superimposed on the intermolecular forces of some portion of the molecules selected randomly in the material. Although current study is mainly for the external field induced crystallization of amorphous argon, coming research will be concentrated on that of silicon, which will make a contribution to the advances in the fabrication of polycrystalline silicon (poly-Si) from amorphous silicon (a-Si) at low temperatures.

Efficient fabrication technology of poly-Si thin-film transistors (TFT) at a low temperature has long been demanded and developed for use in photovoltaics, microelectronics, and display devices of larger area and high-quality, since a low temperature process overcomes problems involved in a-Si TFTs and poly-Si TFTs fabricated at a high temperature [1-2]. There are several processes practically available to fabricate poly-Si thin film at low temperatures, including PECVD (plasma enhanced chemical vapor deposition), MIC (metal induced crystallization), ELC (Eximer laser crystallization), PRTA (pulsed rapid thermal annealing), etc. [2-4].

Very recently, it has been shown that an alternating magnetic induction process can bring about a more effective crystallization of a-Si on a glass substrate at temperatures below 500 °C, which promises the crystallization of larger areas and faster processing without problems involved in current fabrication methods such as metal contamination and longer process times [5]. However, mechanisms for the alternating magnetic field crystallization (AMFC) as well as for the MIC are not clearly understood

yet. It can be conjectured that the AMFC is due to heating of a-Si by eddy current losses in an alternating magnetic field or due to field-enhanced oscillation or movement of defects or ions. Heating due to eddy current loss is considered not to be relevant, since it is almost impossible to heat up the a-Si film without heating the glass substrate except using the ELC technique and the process temperature below 500 °C is too low to increase easily the temperature of a-Si film up to effective annealing temperatures for solid-phase crystallization. The second hypothesis that field-enhanced molecular movements may result in global crystallization will be evaluated in this study to optimize the control parameters for the process. In addition, it is shown that metal concentration in the material and external electric field strength are the most important factors for the MIC [3]. There are, however, not many theoretical tools available to examine the second hypothesis. Therefore, the MD technique is selected to determine whether externally forced molecules will cause crystallization, although the forced molecules are selected randomly and the external forces are artificially imposed.

The MD technique is known to have a capability of providing very detail information on the crystallization and nucleation processes and providing critical tests of analytical theories or unexplained phenomena [6-7]. Researches on crystallization using MD simulation include the investigation of the influence of artifacts due to periodic boundary conditions and small size systems, formation of critical nuclei, phase separation, and the comparison of the process with the classical nucleation theory [6, 8-12]. Recently, Caturla et al. [13], Weber et al. [14], and Motooka [15] showed that MD simulation is a useful tool to study the microscopic process of Si crystallization and amorphization induced by ions and defects.

There are, however, few reports available to investigate the external field induced crystallization using MD techniques, which will be applied to examine the second hypothesis for the AMFC process. For simplicity it is assumed that an externally oscillating force with a dc bias is imposed on some portion of molecules chosen randomly. The progress of crystallization at constant temperature are observed through the radial distribution functions, while there are some other tools available such as observing the structure factor and conducting voronoi analysis [6, 11].

SIMULATION METHOD

In order to monitor the external field induced crystallization process of amorphous solid or supercooled liquid as it evolves from its initial to final states, the well-known Lennard-Jones (LJ) 12-6 pair potential has been applied in this MD simulation, given as

$$\Phi(r_{ij}) = 4\mathbf{e} \left[\left(\frac{\mathbf{s}}{r_{ij}} \right)^{12} - \left(\frac{\mathbf{s}}{r_{ij}} \right)^6 \right], \quad (1)$$

The LJ fluid is assumed to be argon and its parameters are as follows: the length parameter $\mathbf{s} = 0.34nm$, the energy parameter $\mathbf{e} = 1.67 \times 10^{-21}J$, and the molecular mass $m = 6.63 \times 10^{-26}kg$. The LJ potential is truncated to zero for distances larger than $2.5\mathbf{s}$ for the expedition of the calculation, while actual potential is infinite in range. The equation of motions are solved by the widely-used “velocity Verlet” algorithm [16] with

a time-step of 5 fs, or $\Delta t^* = 2.335 \times 10^{-3}$. In this work all quantities with an asterisk are nondimensionalized with respect to \mathbf{s} , \mathbf{e} , and m .

Before the simulation for an isothermal crystallization process, a crystalline fcc structure is designed and placed at the center of the computation domain ($L_x^* \times L_y^* \times L_z^* = 9.5 \times 9.5 \times 9.5$), in which molecular number density is 1.001 at $T^* = 0.496$ below the triple point of argon, $T^* = 0.693$. Here L^* denotes the size of the domain in x, y, and z directions. To effectively obtain the amorphous structure the calculation domain is expanded by 0.2 % and its temperature is raised up to $T^* = 2.48$, which is much higher than the experimental value of critical temperature of argon, $T^* = 1.085$. After 100000 time-steps, the system is equilibrated in a supercritical state and thus in an amorphous structure. This amorphous fluid is suddenly cooled down to temperature $T^* = 0.496$ by velocity scaling in the computation domain expanded in the z direction ($L_x^* \times L_y^* \times L_z^* = 9.5 \times 9.5 \times 28.5$). This supercooled liquid undergoes another equilibration process of 100000 steps. After this preprocessing, the equilibrated amorphous structure at temperatures below its triple point is obtained and will be used in this numerical experiment. In the simulation, velocity scaling is performed at each step to make sure that the system is maintained at the designed temperature, $T^* = 0.496$, since the crystallization process will accompany the temperature increase with the expense of potential energy if it were not for velocity scaling for an isothermal condition. The structure of the system is monitored and clarified using the radial distribution function (RDF) at each time step.

The RDF measures how atoms organize themselves around one another [17] and is formulated as

$$\mathbf{r}^* g(\bar{r}^*) = \frac{1}{N} \left\langle \sum_i^N \sum_{j \neq i}^N \mathbf{d}[\bar{r}^* - \bar{r}_{ij}^*] \right\rangle \quad (2)$$

where N is the total number of atoms, \mathbf{r}^* is the number density, and the angular brackets represent a time average.

RESULTS AND DISCUSSION

A crystalline structure obtained from the fcc structure of solid argon is equilibrated at $T^* = 0.496$ as shown in Fig. 1(a), where the crystalline molecular structure is obviously described, although the molecular positions are slightly displaced from their perfect crystalline lattice points due to the thermal agitation. The RDF, $\mathbf{r}^* g(r^*)$, at $T^* = 0.496$ is calculated using Eq. (2) and shown in Fig. 1(b) with the comparison of the reference RDF of the fcc lattice. Although the intensities of peaks for the crystal at $T^* = 0.496$ are much smaller than those of the reference fcc, the tendencies are quite similar to those of the reference.

The temperature of the crystalline argon equilibrated at $T^* = 0.496$ is suddenly raised up to $T^* = 2.48$ beyond its critical temperature and the volume has been slightly expanded to easily attain the amorphous structure and to prevent the molecules from being gasified if the volume expansion becomes large. This amorphous structure is again

cooled down to $T^* = 0.496$ to obtain an amorphous structure at a temperature lower than its triple temperature. This supercooled structure is equilibrated at $T^* = 0.496$ over 100000 time-steps and the molecular distribution is shown in Fig. 2(a). The RDF's for these processes are compared in Fig. 2(b), where the dotted line is for the equilibrated crystalline structure at $T^* = 0.496$, the dashed line for the supercritical fluid at $T^* = 2.48$, and the solid line for the amorphous solid at $T^* = 0.496$. It is clear that the second, fifth, and seventh peaks in the RDF for the crystalline structure are smoothed out in those for amorphous structures and that the third and fourth peaks of the crystalline structure merge into the second peak of amorphous structures. Therefore, the appearance of the second and fifth peaks or the disengagement of the third peak from the fourth peak will be one of signals indicating the initiation of global crystallization process.

To investigate the crystallization phenomena due to external fields, a sinusoidal force with a dc bias is imposed on a certain portion of molecules in the amorphous structure in addition to the inherent internal force due to their intermolecular potentials in Eq. (1). Practically this force may be applied to susceptor molecules due to direct electric fields, electric fields induced by external magnetic field, or other vibration sources. Since the internal force in the LJ molecules is based on the van der Waals interactions and there does not exist any ion or susceptor in the system, electric fields are not supposed to influence the molecular motions. In this study, however, it is assumed that some molecules are selected randomly as those susceptors that are under the influence of external forces, only to simulate and to observe the crystallization behavior indirectly.

As discussed above, the result from this study might be a clue to mechanisms involved in the crystallization of a-Si to poly-Si whose process is athermal. The artificial

force is estimated from the internal force field experienced by each molecule. Since the potentials of molecules are not at their minimum and the molecules are not in a perfect crystalline position, there always exists a force imbalance, which may be induced by thermal excitation, defects, non-crystalline structures, or other disturbing sources. At each time step, therefore, the forces acting on each molecule by neighboring molecules are averaged and the averaged force is used as the amplitude of the external force. This averaged force decreases as initially amorphous material undergoes a crystallization, which is not shown in this work. The external force acting on susceptible molecules is modeled as

$$F_{ext}^* = A^*[\cos(\omega^* t^*) + B^*]/(1 + B^*), \quad (3)$$

where A^* is based on the averaged force and B^* is the dc bias for the oscillation.

Another parameter to be determined is the period of the externally induced vibration. Representative periods are estimated from the Debye frequency of argon [18] and the natural frequency of the LJ potential linearized as a harmonic potential, which are 521.6×10^{-15} sec and 1781×10^{-15} sec, respectively. These characteristic periods are very close to each other and can be expressed in terms of simulation time-steps of 104 and 356, respectively. Based on these periods, cyclic forces are imposed on susceptor molecules selected randomly from the system.

Figure 3 compares the potential variation during the crystallization with those of crystalline and amorphous states. In this simulation the force constant, A^* in Eq. (3) is 1.5 times the averaged force, B^* is 0.5, the period is 10400 time-steps. In this simulation,

the number of susceptors is 5 out of the total 864 molecules. While the potential variation for amorphous and crystalline structures fluctuate about their mean values, the potential during crystallization decreases from the values of amorphous to those of crystalline states with a sinusoidal fluctuation synchronized to the external cyclic-force. It can be understood that the structure has been changed from amorphous to crystalline states, but the initiation of crystallization cannot be easily detected from this potential variation.

Figure 4 shows the variation of the RDF's from time step 0 to 62000 for the same case discussed in Fig. 3. The RDF at time step 0 is for amorphous structure after 100000 steps equilibration period of the supercooled liquid, in which the second peak is not shown and the third and fourth peaks are merged into one peak. Around time step 30000 the second peak starts to appear and the third peak does to disengage from the fourth peak. These behaviors become very clear at step 40000. After time step 50000 the shape of the RDF becomes very close to that for crystalline structure. Especially, appearances of the second and third peaks are remarkable in the incipient stage of crystallization. The abrupt increases of those peaks are clearly and simultaneously detected near 40000 steps, which imply that the material is undergoing a global crystallization process, although the creation or destruction of crystalline nuclei cannot be detected. In order to observe the nucleation characteristics in detail an analysis should be conducted based on voronoi polyhedron [6], which is not included in this study. The molecular distributions during this crystallization process are shown in Fig. 5 according to various time steps. While any regular structure has not been shown up to 25000 steps, the crystallization structure starts to grow around time step 30000 and completes around step 50000, which can be

recognized in Fig. 4. In addition, this crystallization process can be estimated from the appearances of the second and third peaks are described in Fig. 6 with respect to time. The abrupt increases of those peaks are clearly and simultaneously detected near 40000 steps, which imply the beginning of a global crystallization process. Comparing to the variation of potentials shown in Fig. 3, the variations of the second and third peaks are prominently clear during crystallization process.

Based on these sudden jumps of the second and third peaks in the RDF as a crystallization criterion, Fig. 7 shows the domain for the crystallization delay with respect to the number of susceptor molecules imposed by external forces out of the total 864 molecules. The crystallization delay decreases as the number of susceptor molecules increase. Note that even one susceptor can induce the global crystallization, although the delay is comparatively large. However, the case of the susceptor number greater than 16 out of 864 molecules cannot have the well-crystallized structure similar to the structure shown in Fig. 5. The molecular structure after 500000 steps and RDF's variation with respect to time are shown in Fig. 8 for the case of 20 susceptors. As discussed in Fig. 7 too many susceptor molecules may hamper the effective global crystallization. Although the intensity of the first peak becomes significantly large and the third peak is disengaged from the fourth peak, the second peak has not been shown. It can be implied that {111} structure has been accomplished very locally, while {100} structure cannot be induced due to the large movement of the susceptor molecules.

Figure 9 shows the effect of dc bias on the crystallization for 5 susceptors and $A^* = 1.0$. Crystallization cannot be possible with pure sinusoidal forces for this simulation up to 500000 steps and it is very effective for crystallization to have a dc bias superposed

to cyclic fields. Although it cannot be said that a pure cyclic field cannot induce global crystallization from these simulations, it is found that a cyclic field with a dc bias can decrease the crystallization delay significantly and this concept can be applied to low-temperature crystallization processes such as AMFC, MIC, etc.

Figure 10 shows the effect of the force coefficient, A^* , on the crystallization for 5 susceptors and $B^* = 0.5$. The effective range for crystallization lies near the average force experience by each molecule.

Although the crystallization in this study may be somewhat influenced and expedited by the artifacts of periodic boundary conditions and small number of molecular system, it has been shown that an effective crystallization can be achieved under the influence of external cyclic force fields, especially with a dc bias, comparing the behavior of molecules without external fields.

CONCLUSIONS

Using molecular dynamics technique, we have investigated an isothermal crystallization process of an amorphous structure of argon owing to an external cyclic force-field with a dc bias.

Through comparisons of the radial distribution functions (RDF) for crystalline and amorphous states, the degree of crystallization can be estimated. An abrupt increase of the second and third peaks in RDF is observed during the process, which occurs simultaneously with the steepest decent of potential energies.

While even a small number of susceptor molecules can induce crystallization, a large number of susceptors cannot induce global crystallization effectively. It is shown that the crystallization process becomes more efficient when the external cyclic force is shifted by a dc bias, while crystallization cannot be achieved easily without a dc bias. The optimal value of the amplitude of the external cyclic force is close to the averaged force experienced by each molecule.

Although the external forces acting on molecules are artificially designed, the behavior of susceptor molecules under the influence of electric, magnetic fields, or other vibration sources can be indirectly observed and thus this crystallization process would explain the mechanisms involved in the AMFC or MIC at low temperatures.

REFERENCES

1. T. Sameshima, "Status of Si Thin Film Transistors," *J. Non-Crystalline Solids*, V. 227-230, pp. 1196-1201, 1998.
2. T.E. Dyer, J.M. Marshall, W. Pickin, A.R. Hepturn, and J.F. Davies, Polysilicon Produced by Excimer (ArF) Laser Crystallization and Low Temperature (600 °C) Furnace Crystallization of Hydrogenated Amorphous Silicon (a-Si:H), *J. Non-Crystalline Solids*, vol. 164-166, pp. 1001, 1993.
3. S.Y. Yoon, S.J. Park, K.H. Kim, and J. Jang, Metal-Induced Crystallization of Amorphous Silicon, *Thin Solid Films*, vol. 383, pp. 34-38, 2001.
4. Y. Zhao, W. Wang, F. Yun, Y. Xu, X. Liao, Z. Ma, G. Yue, and G. Kong, Polycrystalline Silicon Films Prepared by Improved Pulsed Rapid Thermal Annealing, *Solar Energy Materials & Solar Cells*, vol. 62, pp. 143-148, 2000.

5. S.H. Park, J.S. Lee, Y.K. Choi and H.J. Kim, Nonthermal Crystallization of Amorphous Solid Materials, *Proceedings of Colloquium on Micro/Nano Thermal Engineering*, Seoul National University, Seoul, Korea, pp. 233-256, 2002.
6. W.C. Swope and H.C. Anderson, 10^6 – Particle Molecular-Dynamics Study of Homogeneous Nucleation of Crystals in a Supercooled Atomic Liquid, *Physical Review B*, vol. 41, No. 10, pp. 7042-7054, 1990.
7. M.P. Allen and D.J. Tildesley, *Computer Simulation of Liquids*, Oxford, 1987.
8. M.J. Mandell, J.P. McTague, and A. Rahman, Crystal Nucleation in a Three-Dimensional Lennard-Jones System. II. Nucleation Kinetics for 256 and 500 Particles, *J. Chem. Phys.*, vol. 66, pp. 3070-3075, 1977.
9. M. Tanemura, Y. Hiwatari, H. Matsuda, T. Ogawa, N. Ogita, and A. Ueda, Geometrical Analysis of Crystallization of the Soft-Core Model, *Prog. Theor. Phys.* vol. 58, pp. 1079-1095, 1977.
10. J. X. Yang, H. Gould, W. Klein, Molecular Dynamics Investigation of Deeply Quenched Liquids, *Physical Review Letters*, vol. 60, No. 25, pp. 2665-2668, 1998.
11. M.J. Mandell, J.P. McTague, and A. Rahman, Crystal Nucleation in a Three-Dimensional Lennard-Jones System: A Molecular Dynamics Study, *J. Chem. Phys.*, vol. 64, pp. 3699-3702, 1976.
12. S. Pickering and I. Snook, Molecular Dynamics Study of the Crystallization of Metastable Fluids, *Physica A*, vol. 240, pp. 297-304, 1997.
13. M.J. Caturla, T. Diaz de la Rubia, G.H. Gilmore, Recrystallization of a Planar Amorphous-Crystalline Interface in Silicon by Low Energy Recoils: A Molecular Dynamics Study, *J. Appl. Phys.*, vol. 77, pp. 3121-3125, 1995.

14. B. Weber, K. Gartner, D.M. Stock, MD-Simulation of Ion Induced Crystallization of Amorphization Process in Silicon, *Nuclear Instruments and Methods in Physics Research B*, vol. 127/128, pp. 239-243, 1997.
15. T. Motooka, Molecular Dynamics Simulations for Amorphous/Crystalline Si Interface: Amorphization and Crystallization Induced by Simple Defects, *Nuclear Instruments and Methods in Physics Research B*, vol. 127/128, pp. 244-247, 1997.
16. W.C. Swope, H.C. Anderson, P.H. Berens, and K.R. Wilson, A Computer Simulation Method for the Calculation of Equilibrium Constants for the Formation of Physical Clusters of Molecules: Application to Small Water Clusters, *J. Chem. Phys.* vol.76, pp. 637-649, 1982
17. J.M. Haile, *Molecular Dynamics Simulation*, John Wiley & Sons, pp. 260-267, 1992.
18. C. Kittel, *Introduction to Solid State Physics*, 7th Ed., John Wiley & Sons, p. 126, 1996.

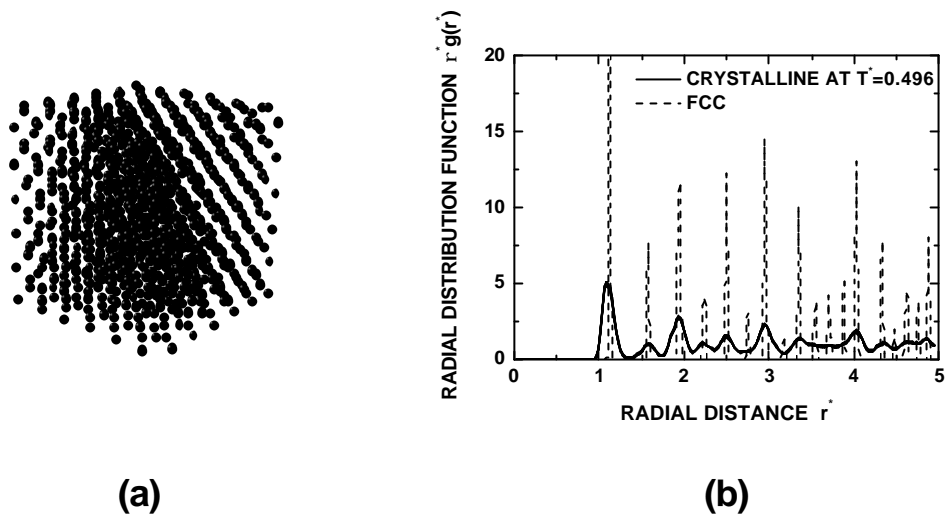


Figure 1. (a) Molecular distribution for crystalline structure and (b) radial distribution functions for fcc and crystalline structures at $T^* = 0.496$.

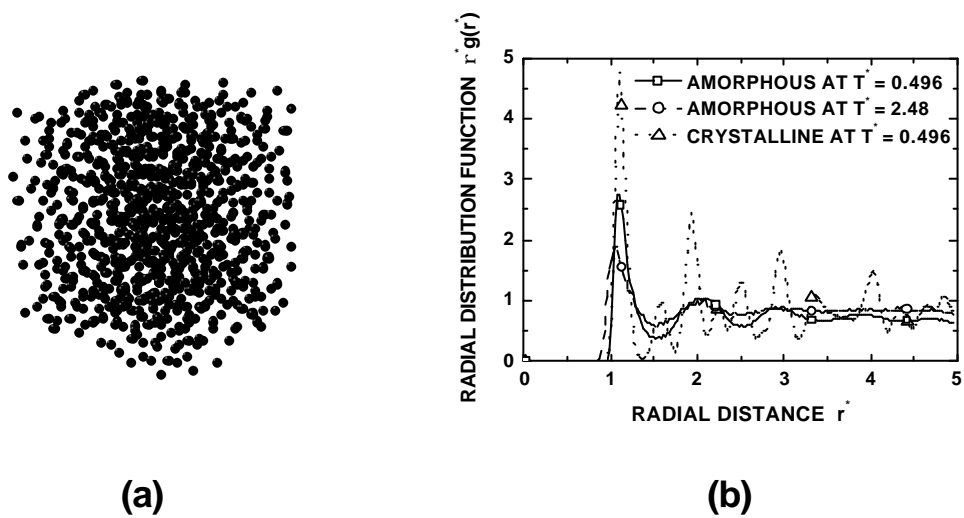


Figure 2. (a) Molecular distribution for amorphous structure and (b) radial distribution functions for crystalline structure at $T^* = 0.496$ and amorphous structures at $T^* = 0.496$ and 2.48 .

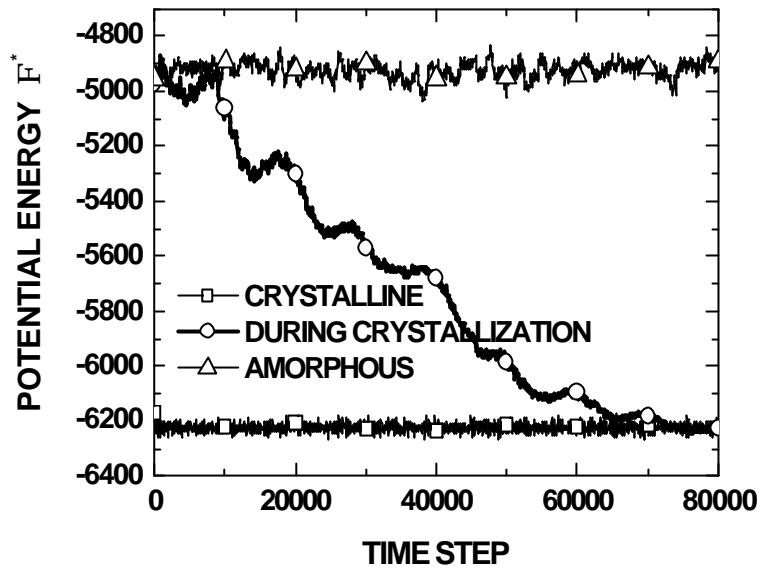


Figure 3. Comparison of potential energy during crystallization to those for crystalline and amorphous states at $T^* = 0.496$.

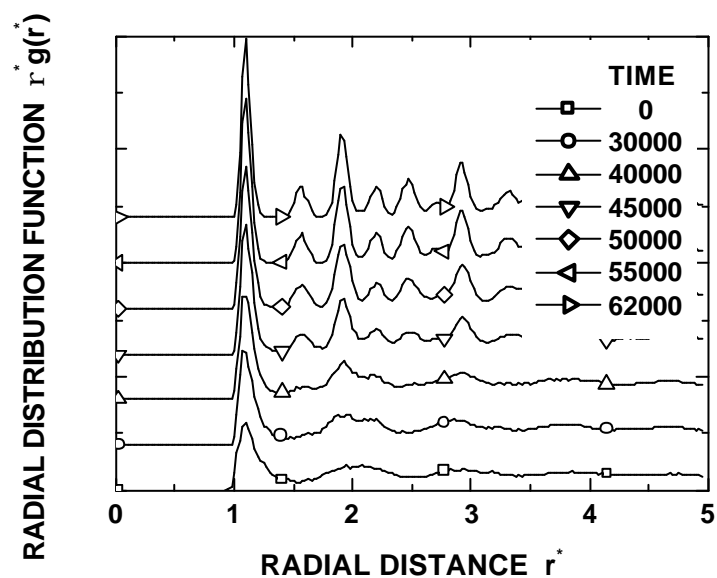
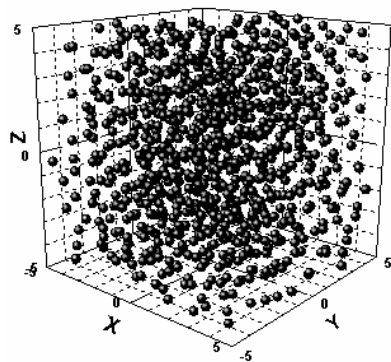
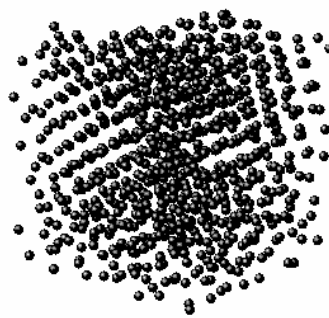


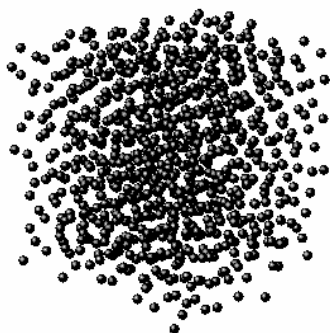
Figure 4. Radial distribution functions during crystallization for various times at $T^* = 0.496$.



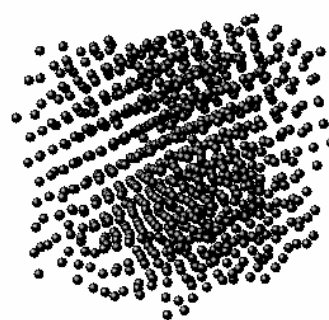
Time Step 25000



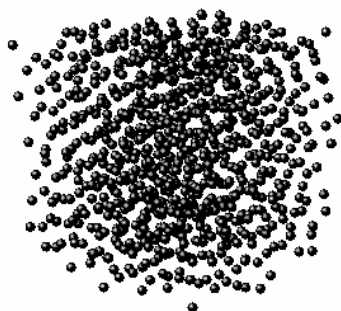
40000



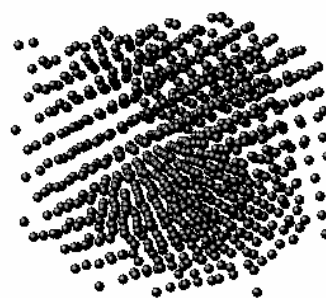
30000



45000



35000



50000

Figure 5. Molecular distributions during the crystallization process induced by an external force-field.

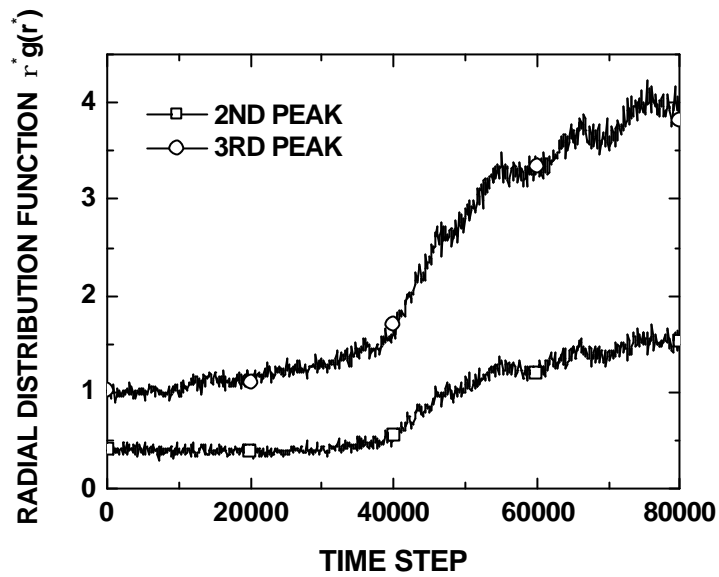


Figure 6. The second and third peaks in radial distribution functions during the crystallization process at $T^* = 0.496$.

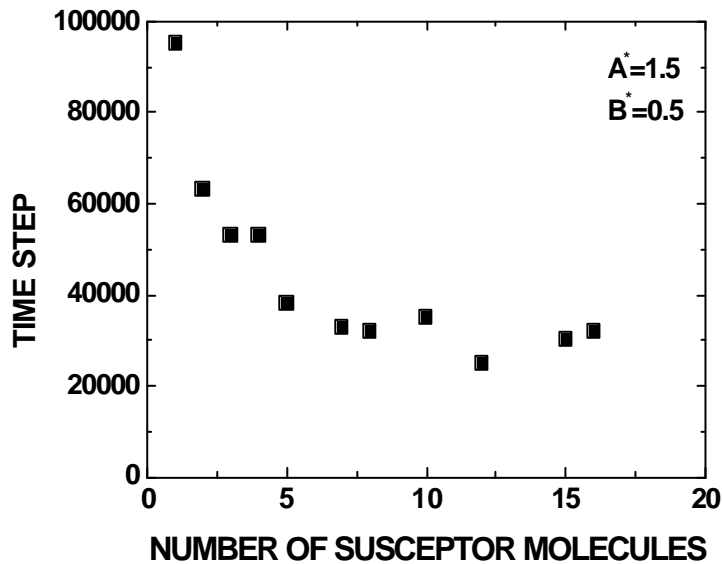


Figure 7. Time steps for incipient stages of the crystallization process at $T^* = 0.496$ with respect to the number of susceptor molecules.

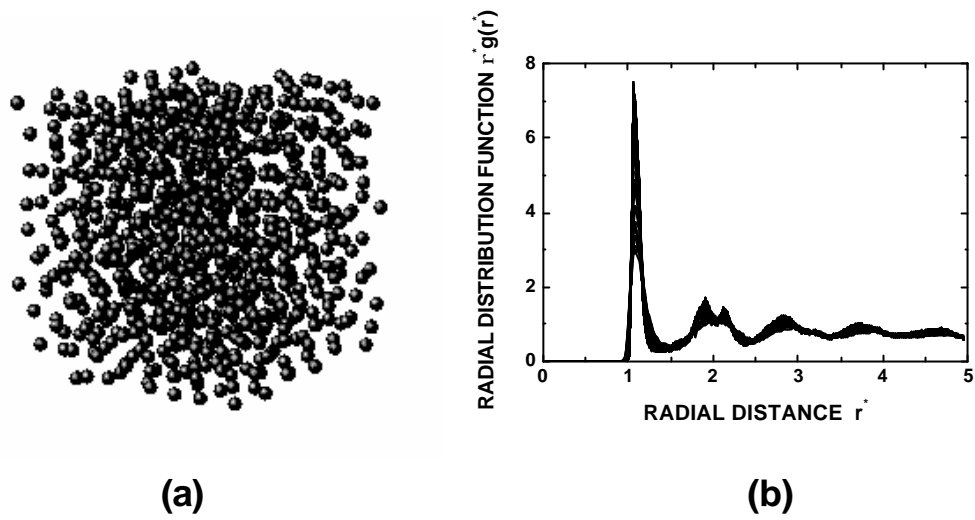


Figure 8. (a) Molecular distribution and (b) radial distribution functions for the crystallization process with the susceptor numbers of 20.

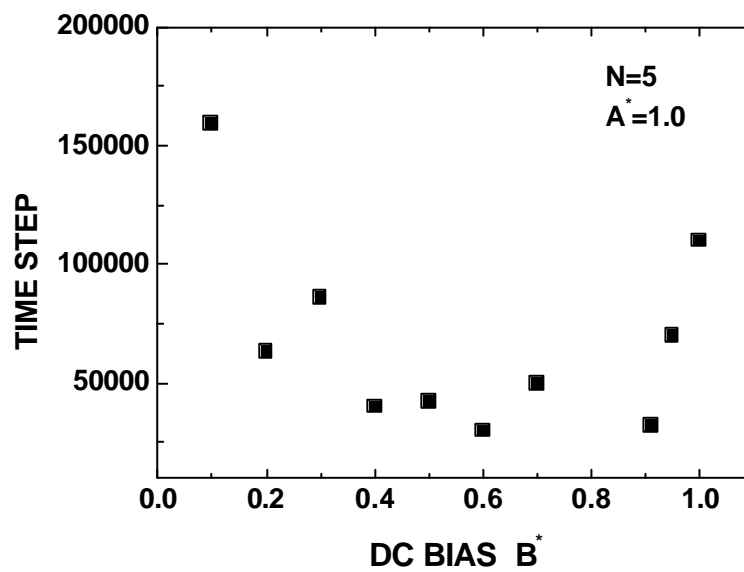


Figure 9. Time steps for incipient stages of the crystallization process at $T^* = 0.496$ with respect to dc bias.

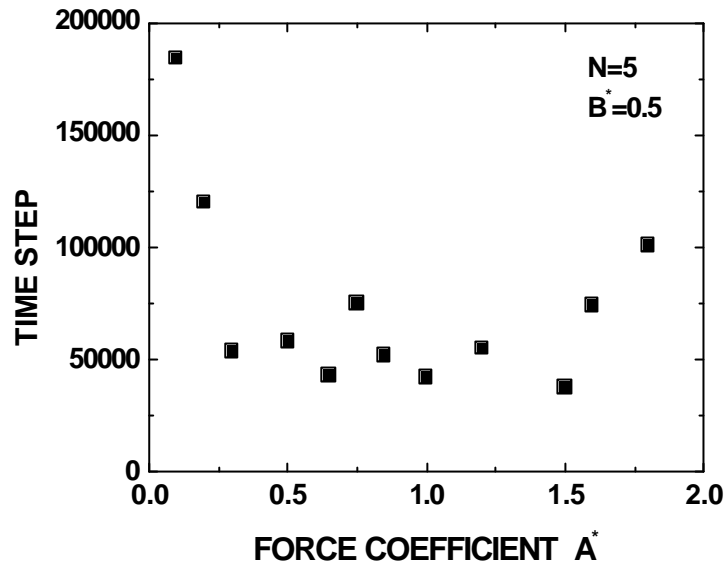


Figure 10. Time steps for incipient stages of the crystallization process at $T^* = 0.496$ with respect to force coefficient.